

Generation of high-saturation two-level iridescent structures by vibration-assisted fly cutting

Yupeng He^a, Tianfeng Zhou^{a,*}, Xiaobin Dong^a, Peng Liu^a, Wenxiang Zhao^a, Xibin Wang^a, Yao Hu^b, Jiwang Yan^c

^a Key Laboratory of Fundamental Science for Advanced Machining, School of Mechanical Engineering, Beijing Institute of Technology, No. 5 Zhongguancun South Street, Haidian District, Beijing 100081, PR China

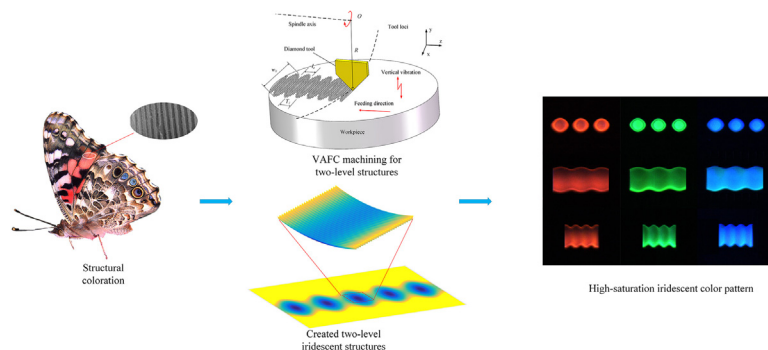
^b Beijing Key Laboratory for Precision Optoelectronic Measurement Instrument and Technology, School of Optics and Photonics, Beijing Institute of Technology, No.5 Zhongguancun South Street, Haidian District, Beijing 100081, PR China

^c Department of Mechanical Engineering, Faculty of Science and Technology, Keio University, Yokohama 223-8522, Japan

HIGHLIGHTS

- Two-level structures consisting of the first-order and second-order features are designed to induce iridescent structures.
- Vibration-assisted fly cutting (VAFC) was proposed to generate two-level iridescent structures in a single step.
- A VAFC platform and an optical detection system are developed to fabricate and test the iridescent two-level structures.
- The regulated two-level structures with high saturation and uniformity have potential application in functional decoration.

GRAPHICAL ABSTRACT



ARTICLE INFO

Article history:

Received 28 April 2020

Received in revised form 21 May 2020

Accepted 30 May 2020

Available online 01 June 2020

Keywords:

Microstructure

Submicron structure

Two-level structure

Structural color

Iridescence

Vibration-assisted fly cutting

ABSTRACT

The submicron-level structured surface induces viewing-angle-dependent iridescence, and has wide applications in multi-color printing, micro-display projection, invisibility cloak technology. In this study, several types of two-level structures, which consist of the first-order micro geometric features corresponding to the pattern shape and the second-order submicron grooves corresponding to the diffraction grating, are designed to directly induce a variety of iridescent patterns based on their shape regulations. To fabricate these two-level iridescent structures with high accuracy in a single step, vibration-assisted fly cutting (VAFC) is proposed. VAFC involves the low-frequency vibration of the workpiece in the vertical direction during the feed in the horizontal direction and the high-speed rotation of the diamond cutting tool. A 3D theoretical model is established for the numerical simulation of the generating process of the iridescent structures and the regulation of the first-order geometric feature by vibration parameters. As the key parameter to the iridescent color, the spacing of the second-order submicron grooves is flexibly controlled by the feed rate. A VAFC platform is developed to fabricate the two-level structures and an optical detection system is setup to test the surface iridescence. Various vivid colors are regulated by the two-level structures with high saturation and uniformity.

© 2020 The Authors. Published by Elsevier Ltd. This is an open access article under the CC BY-NC-ND license (<http://creativecommons.org/licenses/by-nc-nd/4.0/>).

* Corresponding author.

E-mail address: zhoutf@bit.edu.cn (T. Zhou).

1. Introduction

Structural coloration has drawn significant interest in both academia and industry because of its potential applications in multi-color printing, micro-display projection, and invisibility cloak technology [1–4]. Structural coloration has been attributed to a physical process in which complex interactions between submicron structures and visible light manipulate light propagation [5–7]. The diffraction-grating induced structural coloration exerts an iridescent effect such that the apparent color evidently changes with the observation angle [7–9]. Iridescent color induced by reflection-based diffraction grating has better performance than that induced by transmission-based diffraction grating because it is not affected by materials transmittance [10–12]. This kind iridescent color provides the main way to artificially develop structural color due to its high utilization ratio to visible light.

To fabricate structural coloration and high-efficiently produce structural color patterns, micro-nano manufacturing technologies are developed to machine extremely uniform submicron structures serving as diffraction gratings on surfaces for iridescent coloration. Lithography technologies are traditional approaches to producing high-quality diffraction gratings on molds for mass production of their replicates [13]. These methods can efficiently fabricate unitary microstructure arrays but are not able to generate complex color patterns on curved surfaces. Femtosecond laser technology has been widely applied to induce periodic near-subwavelength ripples on metallic surfaces for structural coloration [14–16]. This technology is well known for its high production, however it produces a semiregular grating which will affect the diffraction effect to the visible light [17,18]. Moreover, the ripple spacing induced by femtosecond laser technology is subject to the wavelength of the laser source and cannot be flexibly regulated in process, which also restricts its application in manufacturing of structural color patterns [1,17,19].

Controllable submicron structures for structural coloration on various material surfaces can be feasibly manufactured and are used to generate color patterns [8,20]. Guo and Yang proposed an ultrasonic modulation machining technique referred to as elliptical vibration texturing (EVT) to generate periodic submicron-scale ripples that function as gratings to achieve an iridescent color. The grating spacing can be flexibly controlled with an appropriate combination of processing parameters, and patterns and images are produced on metallic surfaces by EVT in parallel lines [21,22]. Suzuki and Huang also proposed amplitude-controlled, vibration-assisted machining technology to generate novel patterns by synchronizing the tool vibration amplitude with the tool feed position [20,23]. However, the structural patterns and images induced by EVT have a low resolution because of the severe distortion of the adjacent area between two columns of gratings [8,21]. Moreover, these submicron structures are created pixel-to-pixel to induce structural color patterns and images by a complex tool path planning. Therefore the idea is innovatively and initially proposed in this research that two-level structures with first-order geometric features corresponding to the pattern shape and second-order submicron structures corresponding to the diffraction grating are created to directly induce structural color patterns. Ultra-precision side milling (UPSM) use servo motion to simultaneously generate primary surface and secondary micro/nano structures [24], however it's limited by the low machining efficiency because of the needed many steps during one two-level structures manufacturing. The end-fly-cutting-servo (EFCS) is demonstrated to fabricate hierarchical micro-nanostructures with high efficiency, which shows the good diffraction performance to visible light [25,26]. However, since the second-order submicron grooves distribute on the every rotating circle of fly-cutting tool, EFCS cannot generate fully parallel grooves which will affect the iridescent effect in structural coloration. In addition, the selective local texturing of the whole surface is not feasible for EFCS. To directly fabricate high-quality structural patterns in single step machining, ultraprecision technology for highly regular two-level structures is developed to induce structural coloration.

This paper proposes a mechanical method named vibration-assisted fly cutting (VAFC) to generate two-level structures for iridescent structures, in which the coupling motion of the fly cutting of the diamond tool and the low-frequency vibration with of the workpiece are used to efficiently generate two-level structures. The second-order grooves with controllable spacing serve as micro gratings to induce iridescent color on the workpiece surface. By regulating the processing parameters, two-level iridescent structures with varying geometries can be generated on a machined surface. The proposed technology provides a flexible method for generating two-level iridescent structures with varying shapes and colors, which have potential applications in micro-optics, display devices and functional decoration.

A three-dimensional (3D) simulation model is established to demonstrate the proposed methodology and assist in the design and manufacture of two-level structures. The experimental setup is assembled, and the process principle of VAFC is illustrated. The two-level structure is regulated using appropriate combinations of processing parameters for shape manipulation of the iridescent structures. Finally, the diffraction properties of the two-level iridescent structures are detected using a self-established optical testing device.

2. Methodology

2.1. Principle of the iridescent color generation

Iridescent color results from both the interference and diffraction effects of the reflected light by submicron grooves and it displays that the color evidently changes with the observation angle. The iridescent color relates to the wavelength of diffracted light which depends on both the diffracted light angle and the groove spacing, and can be explained by the grating equation

$$\sin\theta_i + \sin\theta_d = \frac{m\lambda}{d} \quad (m = 0, \pm 1, \pm 2, \dots) \quad \lambda = \frac{d(\sin\theta_i + \sin\theta_d)}{m} \quad (1)$$

where d is the groove spacing; λ is the wavelength of the diffracted light; θ_i and θ_d are the incident angle and viewing angle, respectively; and m is the diffraction order [27]. Angular dispersive power (δ) describes the resolution of diffraction angles for the diffracted light at different wavelengths. It is defined as follows:

$$\delta(\lambda) = \frac{\partial\theta_d}{\partial\lambda} = \frac{m}{d \cos\theta_d} \quad (2)$$

It should be noted that a larger dispersive power means the more obviously iridescent color. According to Eq. (2), at a larger diffraction angle, the iridescent color appears as larger angle between the lines of diffracted light. In addition, reducing the groove spacing can increase the angle between all the spectral lines of diffracted light. According to the grating-diffraction theory, most of the light intensity of diffracted light is distributed in the first order diffraction ($m = 1$) and the groove spacing near the visible-light wavelength ($d \rightarrow \lambda$) increases the light intensity of the diffracted light. The saturation of induced iridescent color will be increased due to the enhanced light intensity. Therefore, to enhance the iridescent effect for structural coloration and improve the iridescent color with a high saturation, the groove spacing should be reduced to the visible wavelength range as much as possible.

Since the iridescent color can only appear where there is submicron groove array, a complex array composed of grooves with varying lengths and depths is initially proposed in this paper, and it will display as a complex colorful pattern due to the iridescent effect. This kind submicron groove array termed two-level structure will be designed with a certain shape and manufactured to generate two-level iridescent structures.

2.2. Vibration-assisted fly cutting

To generate two-level iridescent structures by mechanical machining, the intuitive idea is to periodically modulate the cutting depth of a cutting tool in machining structures. Fly cutting is a potential process for generating grooves because of its high efficiency and the high quality of the machined surface [28–30]. Specifically, workpiece feeding in the spindle-axis direction in fly cutting can generate grooves in the visible spectrum in a single step. During axial-feeding fly cutting, one groove is generated per rotation of the cutting tool, and periodic grooves that serve as gratings are generated by workpiece feeding perpendicular to the rotation plane of the cutting tool. Prompted by modulation cutting, the sinusoidal vibration of workpiece in the vertical direction can be used in axial-feeding fly cutting, which is proposed to generate two-level structures for iridescent structures.

Fig. 1 (a) presents a schematic of VAFC. The workpiece continuously vibrates vertically with controllable frequency (<10 Hz) and amplitude (within a few microns) and feeds in the spindle-axis (Z) direction. Simultaneously, the fly-cutting tool rotates around the axis. The motion of the cutting tool, together with the vibration and feeding of the workpiece, results in a row of two-level structures in single step. The morphology of the two-level structure can be divided into two orders: the first-order micro geometric feature and the second-order submicron structures. The first-order micro geometric feature corresponding to the shape of the iridescent structures is generated by the interference between the tool loci

and the surface of the vibrating workpiece. The second-order submicron structures are grooves with periodically varying depth and spacing, which can serve as gratings to obviously induce iridescence of the proposed two-level structures according to Eqs. (1) and (2).

In axial-feeding fly cutting, the width (w_0) of the groove is determined by both the depth of cut (h) and the rotation radius of the cutting tool (R), which can be expressed as

$$\frac{w_0}{2} = \sqrt{R^2 - (R-h)^2} \tag{3}$$

In VAFC, h and tool displacement (z) are function values that change over time (t) and are given by

$$z = vt \tag{4}$$

$$h = A\sin(2\pi ft + \varphi) + k$$

where A is the amplitude, f is the frequency, and φ is the initial phase of the workpiece vibration, k is the offset distance, which is the distance from the equilibrium position of the relative vibration of the tool to the workpiece to the surface of the workpiece, and v is the feed velocity of the workpiece in the Z direction. The coordinate of the origin in the vertical direction is set when the tool loci lies tangent to the workpiece surface. Derived from Eqs. (3) and (4), the functional relationship between w_0 and z is given by

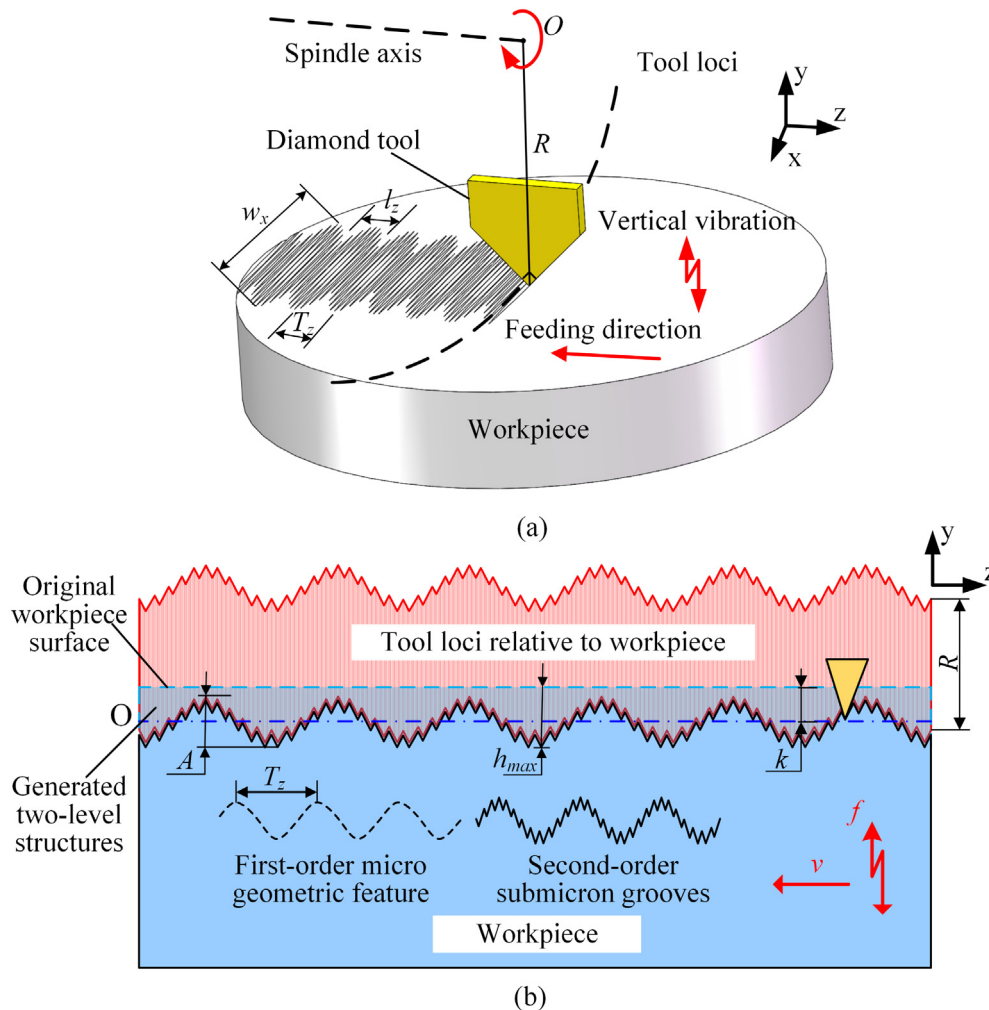


Fig. 1. Schematic of VAFC: (a) process principle, (b) cross-section in the feeding direction of the tool.

$$\frac{w_0}{2} = \sqrt{2(R-k)A \sin\left(\frac{2\pi f}{v}z + \varphi\right) + \frac{A^2}{2} \cos\left(\frac{4\pi f}{v}z + 2\varphi\right) - \left(\frac{A^2}{2} - 2Rk + k^2\right)} \quad (5)$$

which expresses the geometric feature of the two-level structure. The geometric feature is a complex curve but has a definite period. According to Eq. (5), the first-order period (T_z) of the two-level structures can be calculated as

$$T_z = \frac{v}{f} \quad (6)$$

which shows that the first-order period of the two-level structures generated by VAFC is determined by the feed velocity and vibration frequency of the workpiece. In iridescent structure manufacturing, the shape size not only affects the first-order feature of two-level structures but also determines the efficiency for surface grooving. The length (l_z) and width (w_x) of the two-level structures are proposed to characterize the shape size. w_x is equal to w_0 when h is equal to the maximum value h_{max} defined by Eqs. (3) and (4):

$$h_{max} = A + k \quad (7)$$

$$w_x = 2\sqrt{R^2 - [R - (A + k)]^2}$$

Given a fixed rotation radius of the cutting tool, the length of the two-level structure can be controlled by changing the amplitude and offset the distance of the vibration. According to Eq. (7). When the offset distance is less than the amplitude, the length (l_z) of a two-level structure can be determined by solving Eq. (4) when h is 0. However, l_z is equal to the first-order period when the offset distance is greater than the amplitude. l_z is given by:

$$l_z = \begin{cases} \frac{[2 \arcsin(\frac{k}{A}) + \pi]v}{2\pi f} & \arcsin(-\frac{k}{A}) \in [-\frac{\pi}{2}, \frac{\pi}{2}], k > A, k \leq A \\ \frac{v}{f} & \end{cases} \quad (8)$$

Eq. (8) shows that the length of a two-level structure is subject to vibration parameters and feed velocity.

The groove spacing (d) is the second-order period of the two-level structures, which is determined by feed velocity, which can be expressed as

$$d = \frac{v}{n} \quad (9)$$

where n is the rotating speed of the fly-cutting tool.

Fig. 1(b) presents the schematic of a cross-section in the feeding direction of the tool, which illustrates that the two-level structures are

formed because of the periodically regular arrangement of the submicron grooves with varying depths. The mechanism of VAFC indicates that to evidently generate two-level structures, the vibration frequency of the workpiece has to be at least an order of magnitude lower than that of the rotational frequency of the cutting tool. The rotational frequency of the cutting tool typically ranges from 50 Hz to 100 Hz (with a corresponding speed range of 3000–6000 rpm), which implies that the vibration frequency of the workpiece has to be controlled within 10 Hz. A two-level structure can be directly generated per vibration period, so the processing time of one two-level structure is completely dependent on the vibration frequency. The groove spacing of the second-order submicron grooves is determined by the feed velocity of the workpiece.

2.3. Design of the two-level structure for VAFC

To demonstrate the VAFC process, a 3D model for generating two-level structures using the proposed method is established by using Matlab, as shown in Fig. 2. Specifically, to easily establish the model without distortion, the workpiece vibration is regarded as the tool vibration relative to the workpiece in this model. The helicoid rotary surface shows the relative trajectory of fly-cutting tool to the workpiece surface and consists of the compound tool loci. First-order geometric features of the two-level structure are generated at the intersection between the helicoid tool trajectory and the workpiece, and the second-order submicron grooves are generated because of the tool mark and uniformly distributed in the two-level structures.

As investigated in sections 2.1 and 2.2, first-order geometric corresponds to the shape of the iridescent structures and the groove spacing of the second-order submicron structures induces the color of the two-level structures, which achieves that shape and color of the two-level iridescent structure can be controlled independently during VAFC.

To design and manufacture two-level structures, the effects of the vibration parameters on the first-order geometric feature are simulated and predicted using the established model. Fig. 3 shows the simulation analysis when the offset distance of the vibration is solely changed. Fig. 4 illustrates the effects of different offset distances on the two-level structures, and the three different offset distances are 0, A , and $2A$. The horizontal axis represents the workpiece surface, thus the area between the vibration trajectory and the horizontal axis forms as the generated two-level structures. These observations clearly demonstrate the following: offset distance less than A leads to interval two-level structures corresponding to Fig. 4(a); offset distance A leads to adjacent two-level structures corresponding to Fig. 4(b); and offset distance greater than A leads to overlapping two-level structures Fig. 4(c). The offset distance cannot only affect the adjacency forms of the two-level structures but change the size of the structure as well, which is explained in Eqs. (7) and (8). With a change in offset distance, the adjacency form also changes, but the first-order period of the two-level

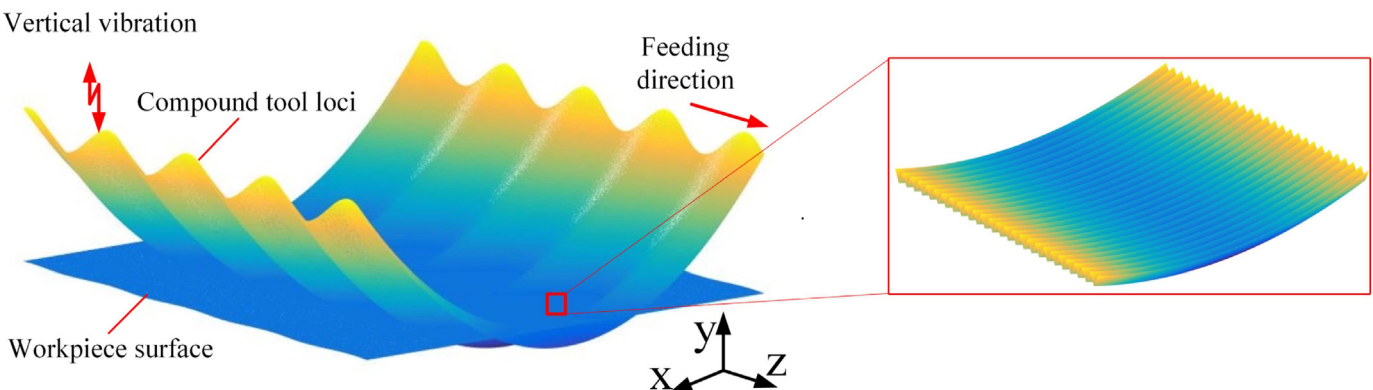


Fig. 2. 3D simulation model for the generation of two-level structures.

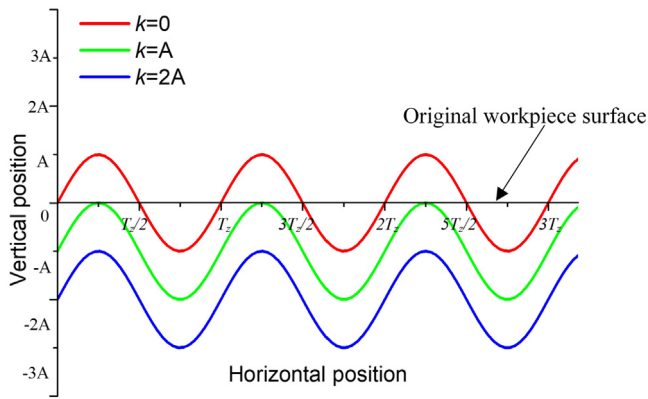


Fig. 3. Simulation analysis of the effect of offset distance.

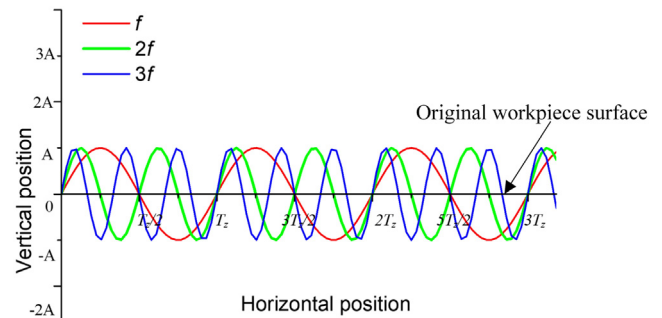


Fig. 5. Simulation analysis of the effect of vibration frequency.

structures remains the same, which shows the consistency of the simulation result in Eq. (6).

The effects of vibration frequency on the geometric feature of the two-level structures are illustrated in Fig. 5. The vibration frequency mainly affects the first-order period of the two-level structures without changing the width of the structures. The number of two-level structures per unit length linearly increases with the frequency, which makes the first-order period decrease. Three different vibration frequencies, f , $2f$ and $3f$ are simulated, as shown in Fig. 6(a), (b) and (c). The simulation results and Eq. (6) demonstrate that the frequency is the most effective method to improve the efficiency for the mass generation of two-level structures on the workpiece surface.

Fig. 7 illustrates the effects of the amplitude on the first-order micro geometric feature of the two-level structures. Similar to the effects of offset distance, a change in vibration amplitude causes the length and width of the two-level structures to change simultaneously but does not affect the period of the two-level structures. Given a non-zero offset distance, three adjacency forms as well as interval, adjacent, and overlapping two-level structures can be generated by regulating the vibration amplitude. When the offset distance is zero, changes in vibration amplitude can only affect the width of the two-level structures and not the length. Fig. 8(a), (b) and (c) illustrate the simulated two-level structures with amplitudes A , $2A$ and $3A$, respectively, when the offset distance is zero. These simulations substantially explain the effects of amplitude on the two-level structures and are consistent with the earlier calculations, which validate the feasibility of the methodology for two-level structures by VAFC.

3. Experimental setup development

3.1. Equipment for two-level structure generation

As analyzed above, the vibration frequency of the workpiece has to be controlled within 10 Hz in VAFC. The low-frequency vibration stage as the key component with controllable vibration frequency is needed. Fig. 9 presents the schematic of the designed vibration stage and its installation diagram. The vibration stage mainly consists of a vibrator, a vertical actuator, and a fixture. The vibrator consists of piezoelectric transducers and provides the designed vibration. The vertical actuator can control the height of the vibrator to precisely adjust the initial height of the workpiece surface. The fixture is designed to clamp the workpiece and connect it with the vibrator. Vertical vibration is achieved by driving the piezoelectric transducer at a low frequency in the vertical direction. The nanoscale positioning and vibration of the vibrator in the vertical direction are regulated by a responsive and high-accuracy controller. The working parameters of the vibration stage are listed in Table 1.

An ultraprecision machine, Nanofom X (Precitech Corporation, USA), is modified for VAFC (Fig. 10). The grooving arbor is coaxially fixed with the spindle to be driven for high-speed rotation. The dynamic balance is adjusted using the equipped balance system of the ultraprecision machine, reducing the peak-to-valley value to <10 nm. The spacing of the proposed submicron grooves is within the visible spectrum, thus a 90° V-shaped cutting tool made from single-crystal diamond is used and mounted in the radius direction at the end of the grooving arbor. The vibration stage is mounted on the B-axis platform of the ultraprecision machine, and the workpiece is clamped with the fixture on the vibration stage. Under the control of the computerized numerical control (CNC) system, the Z-axis with a moving straightness of $0.1 \mu\text{m}/50 \text{ mm}$

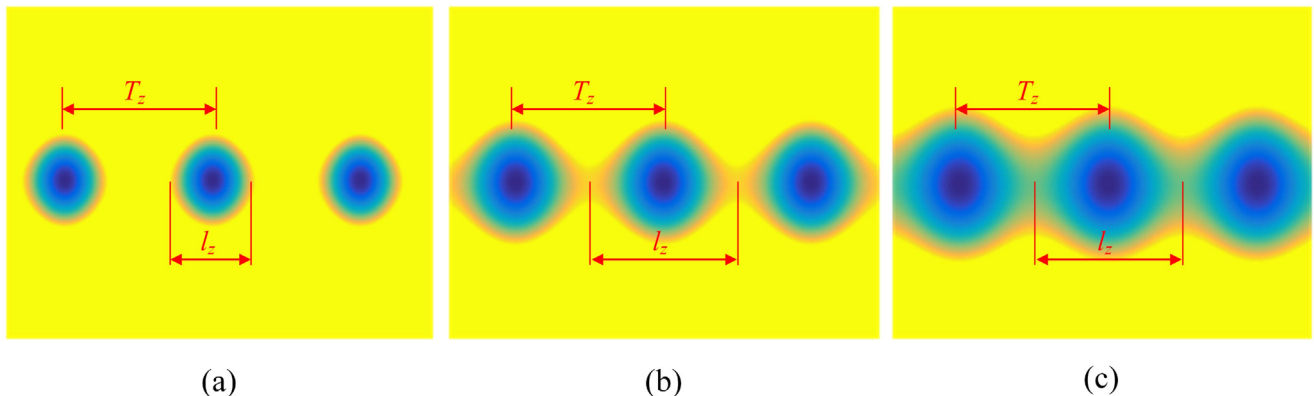


Fig. 4. Two-level structures with different adjacent forms: (a) Interval two-level structures, (b) Adjacent two-level structures, (c) Overlapping two-level structures.

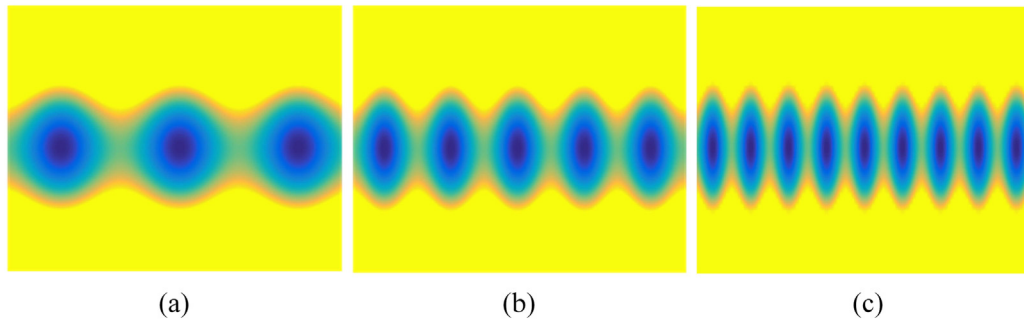


Fig. 6. Two-level structures simulated with different frequencies: (a) Frequency of f , (b) frequency of $2f$, (c) frequency of $3f$.

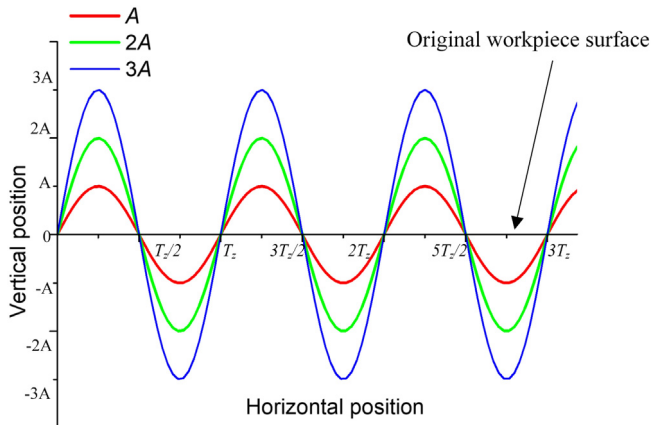


Fig. 7. Simulation analysis of the effect of amplitude.

can contribute to precise workpiece feeding. The programming resolution accuracy of the ultraprecision machine is 0.1 nm. Both tool setting and regulation of the depth of cut are accomplished using the positioning function of the vibration stage.

The frequency and amplitude in VAFC can be controlled via excitation signals, which could be adjusted using the controller. Offset distance is the nominal h and can be controlled using the positioning function of the vibration stage. The feed velocity of the Z-axis, the only parameter to control the groove spacing for iridescent coloration of two-level structures, can be controlled by programming.

The vertical position tolerance of the workpiece surface needs to be controlled <100 nm, and the plane is machined by fly cutting before processing the two-level structures. In planing process, an arc-edge diamond tool (R5) is mounted at the end of the grooving arbor, and the roughness of the plane is kept within 10 nm.

3.2. Optical-test device for two-level structure evaluation

To detect the iridescence of the generated two-level structures, optical-test device was developed as shown in Fig. 11. The white light from the light source is collimated using a collimating lens and was then irradiated on the workpiece surface machined with two-level structures. The diffraction light reflected from the surface transmits through the objective lens, and then is recorded by the image sensor. The machined workpiece was mounted on a two-stage turntable to control the incident angle and viewing angle separately. According to the diffraction equation, the diffracted color is determined by the incident angle, viewing angle, and spacing of the grooves. Given the incident angle and spacing of the grooves, only specific diffracted light can be observed in a specific viewing-angle direction, resulting iridescence. The wavelength of the diffracted light increases with the increase of the viewing angle. To detect the iridescent effect of the two-level structures, the incident angle and spacing of the second-order grooves were held constant.

4. Results and discussions

4.1. Surface morphology in VAFC

The nickel phosphorus (Ni—P) with high-quality and destruction resistance is utilized to manufacture the two-level microstructures, which has been investigated in our previous research [28,31]. The preliminary machined surface with numerous two-level structures is shown in Fig. 12. Manufactured two-level structures on the surface are divided into two groups, the ordinary two-level structures and the two-level iridescent structures, in terms of the spacing of the second-order grooves. Ordinary two-level structures with groove spacing of 3–5 μm cannot present viewing-angle-dependent colors. Whereas, the two-level iridescent structures with groove spacing of 500–800 nm clearly present viewing-angle-dependent colors which is referred to as iridescent colors. In essence, these viewing-angle-dependent colors

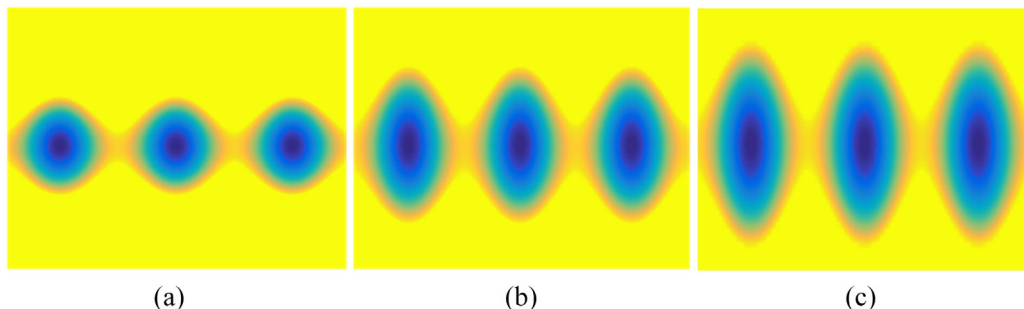


Fig. 8. Two-level structures simulated with different amplitudes: (a) Amplitude of A , (b) amplitude of $2A$, (c) amplitude of $3A$.

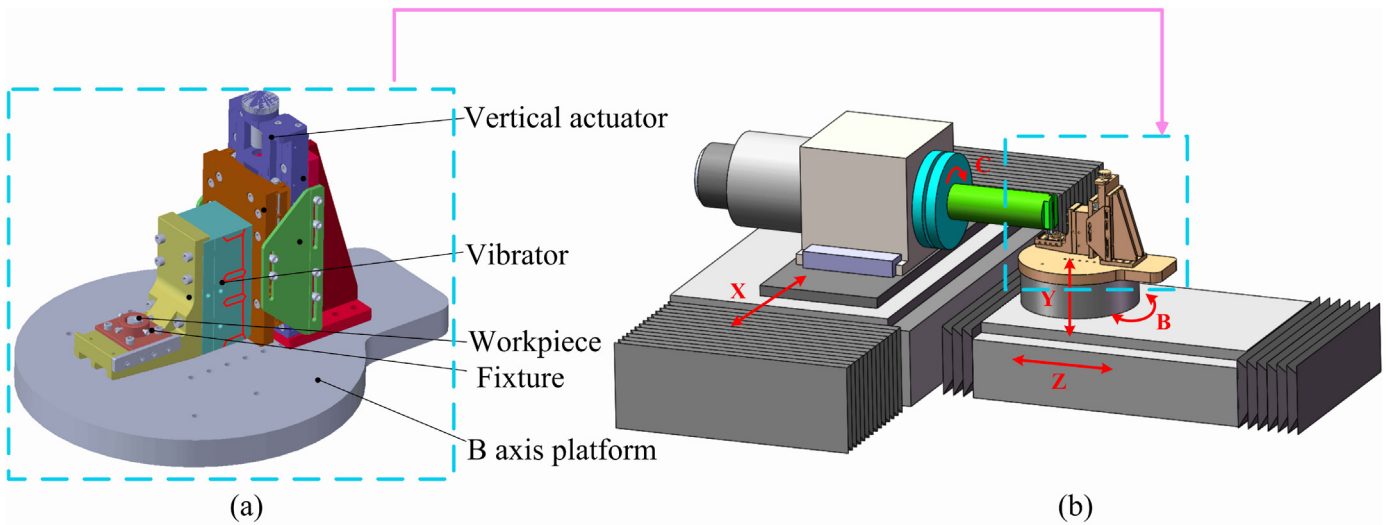


Fig. 9. Schematic of the designed low-frequency vibration stage: (a) designed vibration stage, (b) installation diagram.

Table 1

Working parameters of the vibration stage.

Parameter	Value
Maximum loading (kg)	20
Positioning resolution (nm)	10
Vibration frequency (Hz)	0–10
Maximum amplitude (μm)	20

are attributed to the grating diffraction of the second-order submicron grooves.

Fig. 13(a) presents the several two-level structures produced on the workpiece surface under the following conditions: spindle speed of 3000 rpm, cutting tool rotation radius of 30 mm, feed velocity of

2.1 mm/min, a vibration amplitude of 0.6 μm , and a offset distance of 0 μm . To better investigate the morphology of two-level structure, the vibration frequency is set to 0.05 Hz. The workpiece vibration used is a sinusoidal vibration. A two-level structure was efficiently generated in 20 s, which was determined by the vibration frequency. The first-order micro geometric feature is attributed to the variation in h . The hemiprofile of the first-order micro geometric feature is similar to a sine waveform, which is consistent with the simulation results. According to the simulation results, adjacent two-level structures will be generated if the offset distance equals zero. By contrast, spacing exists between the structures when the offset distance is zero, which originates from a tool-setting error and minimal cutting thickness. To investigate the second-order morphology of the two-level structure, the central area of the two-level structure was measured by scanning

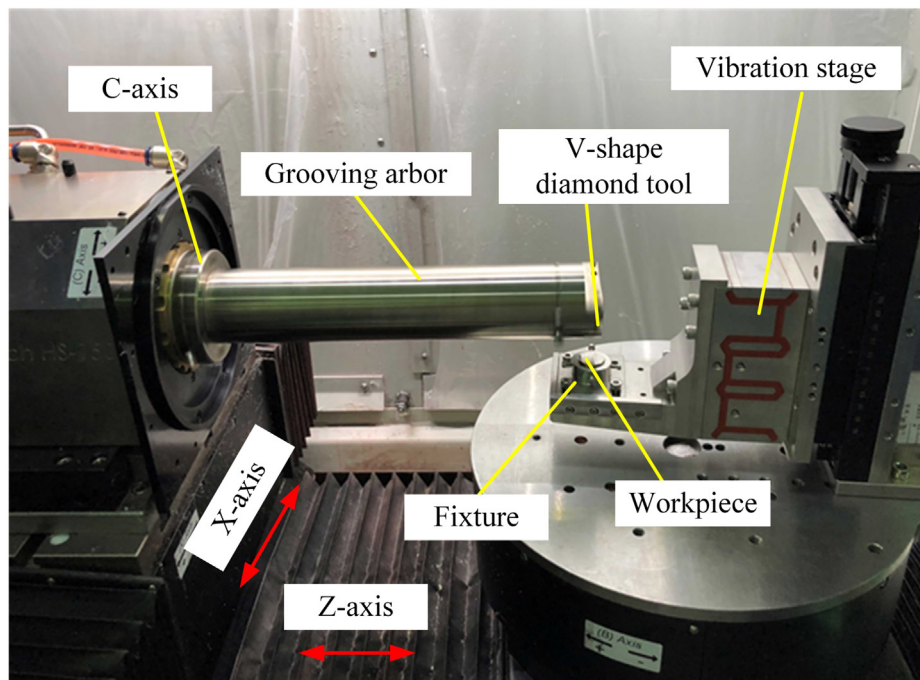


Fig. 10. Photograph of the VAFC platform.

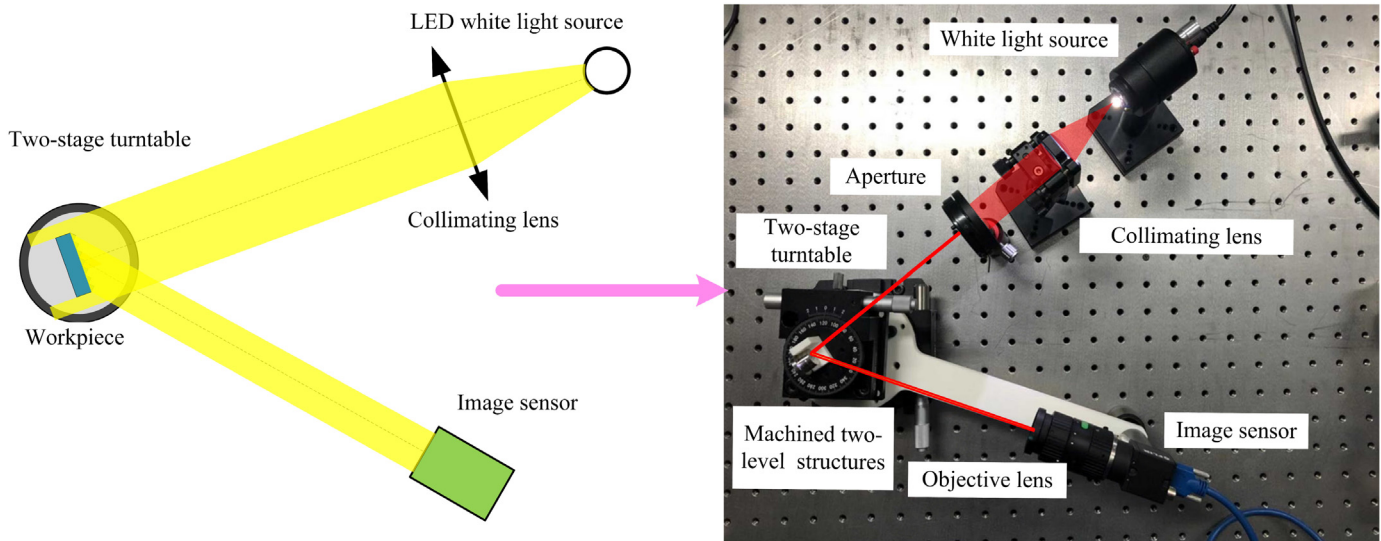


Fig. 11. Optical-test device for the two-level structure evaluation.

electron microscopy (SEM). Fig. 13(b) shows the profile of the second-order submicron grooves using the LEXT OLS5000 (OLYMPUS, Japan). The submicron grooves with high uniformity and quality have an approximate spacing of 700 nm.

As discussed before, the spacing of the second-order submicron grooves can be regulated by the feed rate. The second-order submicron grooves with spacing of 800 nm, 600 nm, 400 nm and 200 nm are created using feed rate of 2.4 mm/min, 1.8 mm/min, 1.2 mm/min and 0.6 mm/min, respectively, as shown in Fig. 14. The spacing range has completely covered the visible spectrum. These machined submicron grooves all have good quality and consistency. The actual spacing is considerably close to the desired value, which indicates its feasibility for controlling groove spacing for iridescent coloration by VAFC. In the submicron-scale machining, the topography accuracy of grooves with bigger spacing is higher than those with smaller spacing. Meanwhile, the grooves with even 200 nm spacing are still high-regularly arrayed and have a high parallelism, which verifies that the experimental setup is dominant in the generation of submicron grooves for structural coloration and the proposed process method and simulation model is feasible for generating two-level iridescent structures.

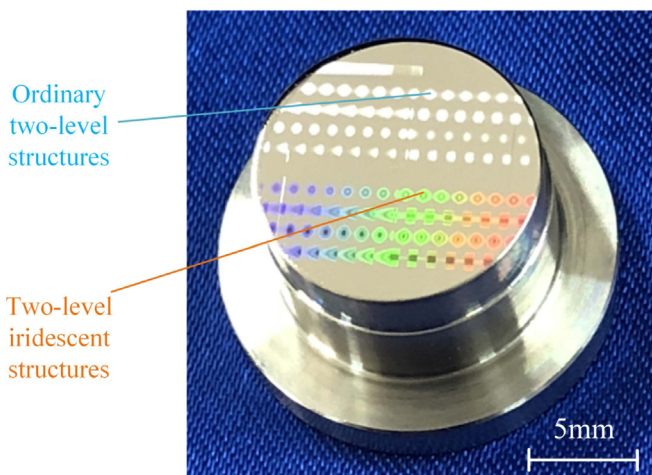


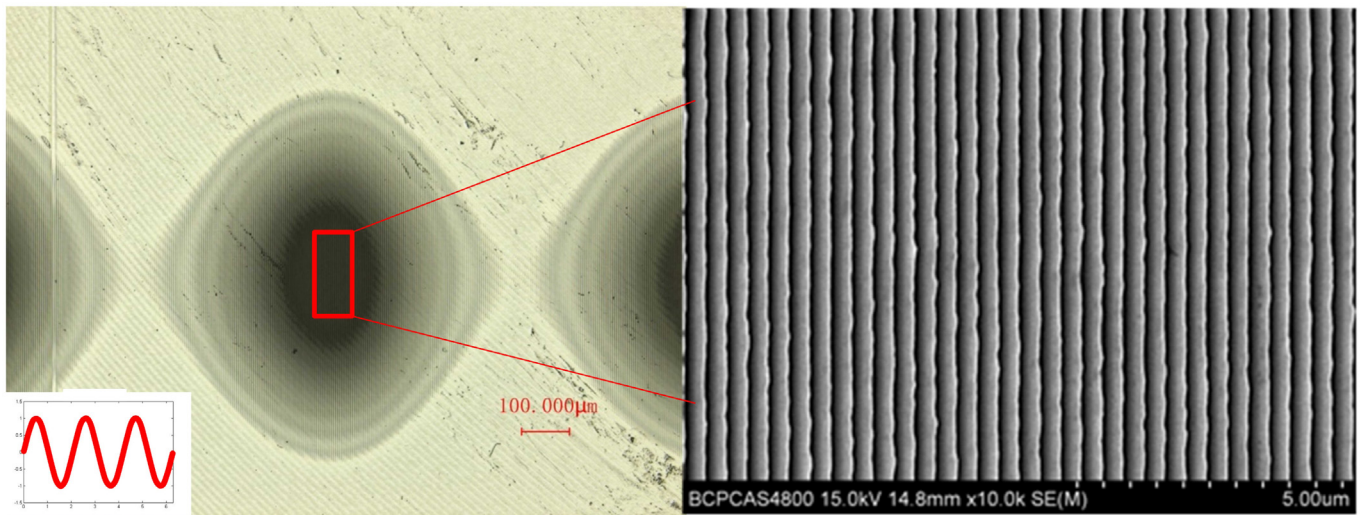
Fig. 12. Fabricated surface with two-level structures.

4.2. Regulation of two-level structures

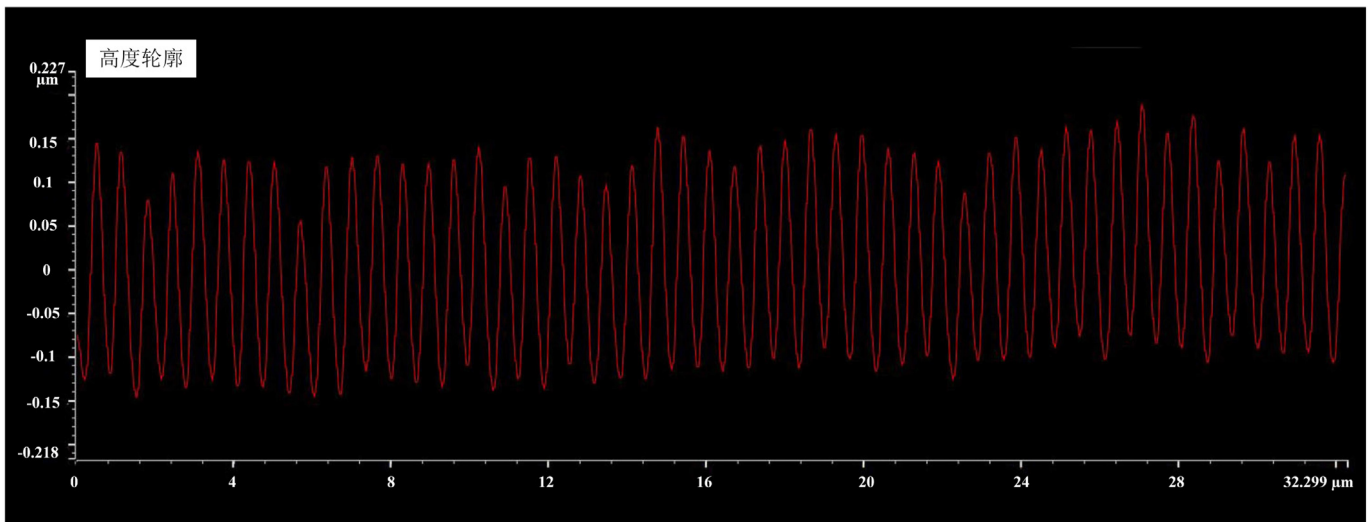
The diffracted color of the two-level structures with definite groove spacing is determined at the fixed incident angle and the viewing angle, so the diffraction color induced by submicron grooves can be regulated by controlling the feed velocity. Regulation of the first-order micro geometric feature can affect the shape of the two-level structures. Thus, the main objective is to regulate shape of the two-level structures for various iridescent structures. Offset distance, vibration frequency, and vibration amplitude are the three key parameters affecting the first-order micro geometric feature, as predicted in simulations. Experiments were conducted under different processing conditions. The sizes of the generated two-level structures were measured (Table 2). The following parameters were applied for all cases: spindle speed of 3000 rpm, cutting tool rotation radius of 30 mm, and feed velocity of 2.1 mm/min.

Fig. 15 shows four groups of generated two-level structures (corresponding to Nos. 1–4 in Table 2), measured with a Keyence microscope (VK-X100) using a laser scanning model. Fig. 15 (a) and (b) show interval two-level structures and overlapping two-level structures produced by VAFC using different offset distances. Interval two-level structures exhibit an isolated distribution of the structures. Meanwhile, overlapping two-level structures are closely linked structures and have a wavy profile. As discussed in Section 2, an offset distance less than the amplitude can induce interval structures, whereas an offset distance greater than the amplitude can induce overlapping structures. As observed from the results, offset distance affects both the length and width of the two-level structure without changing the period, which largely remains consistent with the simulation result.

To evaluate the effects of vibration frequency on the first-order micro geometric feature, a vibration frequency of 1 Hz was used to generate two-level structures by VAFC (Fig. 15(c)). Compared with the 0.05 Hz frequency in Fig. 15(b), the 0.1 Hz frequency halved the first-order period of the two-level structures. As discussed in Section 2.1, the first-order period of the two-level structure is determined by feed velocity and vibration frequency. The feed velocity is kept constant to generate definite spacing of the second-order grooves for the iridescent color. The first-order period of the two-level structures can then be regulated by changing the vibration frequency. Although the first-order period of the two-level structures correspondingly changes with the frequency, the width and adjacency form of the two-level structures remain the same when the other parameters are given and fixed. Therefore, the first-order period of two-level structures can be controlled



(a)



(b)

Fig. 13. Morphology of the two-level structure induced by VAFC: (a) SEM photograph of two-level structure, (b) morphology of the second-order submicron grooves.

with high specificity and efficiency by regulating the vibration frequency.

Control experiments were conducted to investigate the effects of vibration amplitude on the first-order micro geometric feature. The results are shown in Fig. 15(a) and (d). Two different vibration amplitudes, 0.6 μm and 1.8 μm , were used to generate two-level structures while the other parameters are kept constant. These two-level structures are classified as the interval structures because of the offset distances of the two processes being less than their amplitude. In addition, the lengths of the two-level structure in Fig. 15(d) are greater than those in Fig. 15(a) owing to the nonzero offset distance, which is consistent with the simulation results. The width of the two-level structure in Fig. 15(d) is greater than that in Fig. 15(a), which confirms that greater amplitude can increase the width of two-level structures processed by VAFC. The aforementioned analysis indicates that the relative size between the vibration amplitude and offset distance can affect the size and adjacency form of two-level structures. However, the vibration amplitude is easier to control than the offset distance. Therefore, the vibration amplitude is widely used to regulate the adjacency form and size of the two-level structures when the offset distance is first fixed and kept constant during processing.

On the basis of the proposed method, two-level structures were generated on the surface. The effects of the processing parameters on the two-level structures were evaluated, and regulation of the two-level structure was demonstrated by controlling the offset distance, vibration frequency, and amplitude. Regulating the first-order micro geometric feature can be potentially used as an approach to controlling the iridescent structure shapes. The errors between the theoretical and measured sizes of the two-level microstructures were demonstrated to be negligible. These results confirm that the simulation model exhibits high prediction accuracy and can be used to design two-level structures.

4.3. Iridescent color induced by the two-level structure

The generated two-level structures exhibited preliminary iridescence under natural light, which shows the viewing-angle dependence of colors. Two-level iridescent structures were generated, displaying vivid colors. The iridescent colors were attributed to the second-order grooves induced by VAFC. The second-order grooves with varying length and depth served as diffraction gratings, resulting in the iridescence of the two-level structures.

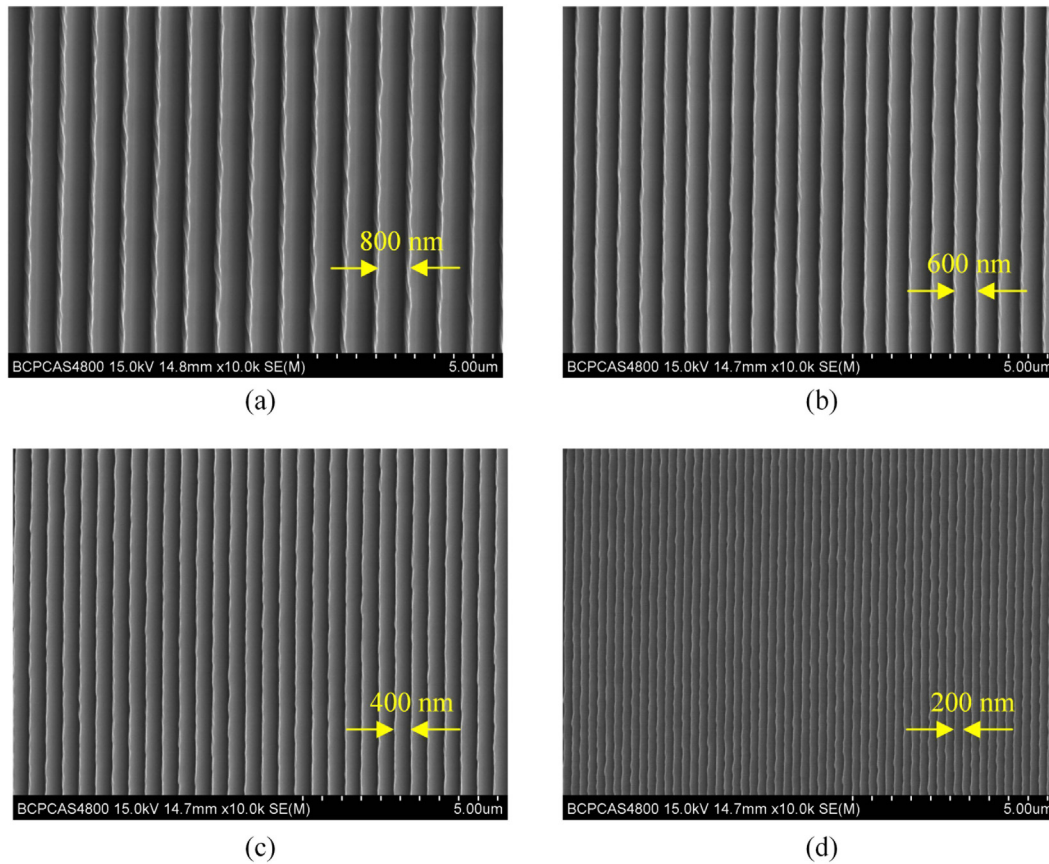


Fig. 14. Second-order submicron grooves with different spacing: (a) 800 nm, (b) 600 nm, (c) 400 nm, (d) 200 nm.

The iridescent effect of the generated two-level structures was detected (Fig. 16). These two-level structures with different geometric features were induced by VAFC with the same feed velocity of 2.1 mm/min. Thus, the second-order grooves of the two-level structures had a spacing of 700 nm. The incident angle of the collimated light was set to 0° and was held constant for all detections. Fig. 16 (a) presents the two-level iridescent structures recorded by the image sensor at a viewing angle of 65° . Iridescent structures with different shapes exhibit the same red color without any coating material and pigment. According to the diffraction equation, given a spacing of 700 nm and an incident angle of 0° , the diffracted wavelength at the viewing angle of 65° is 634 nm, which falls within the red wavelength range of 622–760 nm. The red color was generated at the viewing angle of 65° owing to the iridescent effect. Similar results were obtained at the viewing angles of 55° and 45° , where the diffracted wavelengths calculated at 573 and 495 nm were within the green wavelength range of 500–577 nm and cyan wavelength range of 450–500 nm, respectively. Thus, these two-level structures showed green color [Fig. 16(b)] at the viewing angle of 55° and cyan color [Fig. 16(c)] at the viewing angle of 45° . Moreover, the diffracted light of any wavelength can be caught at a corresponding viewing angle to generate iridescent colors.

The generated iridescent structures at different diffracted angle exhibit high vividness and saturation, and the diffracted color uniformly cover the whole surface of the first-order geometric feature. These findings confirm the excellent color-rendering ability of two-level structures induced by VAFC. The geometric feature of two-level structures can be used to induce varieties of iridescent structures, which can be regulated by controlling the processing parameters. The combinations of these iridescent structures can be inferred to produce complex images, which can be used in anti-counterfeiting, color printing and so on.

5. Conclusion

To directly induce structural color patterns, vibration-assisted fly cutting (VAFC) was proposed to generate two-level iridescent structures. Theoretical analysis, simulations and experiments are conducted to design and fabricate iridescent structures. The iridescent colors of the two-level structures are detected and analyzed. The main conclusions are drawn as follows:

- (1) Low-frequency vibration of the workpiece is introduced in axial-feeding fly cutting to generate two-level structures, including the

Table 2
Effects of VAFC parameters on the types of two-level structures.

No.	k (μm)	f (Hz)	A (μm)	T_z Theoretical /Measured value (μm)	w_x Theoretical/Measured value (μm)	l_z Theoretical/Measured value (μm)
1	0.2	0.05	0.6	700/703	438/435	426/420
2	1.5	0.05	0.6	700/701	710/709	700/701
3	1.5	0.1	0.6	350/348	710/706	350/348
4	0.2	0.05	1.8	700/706	693/685	375/371

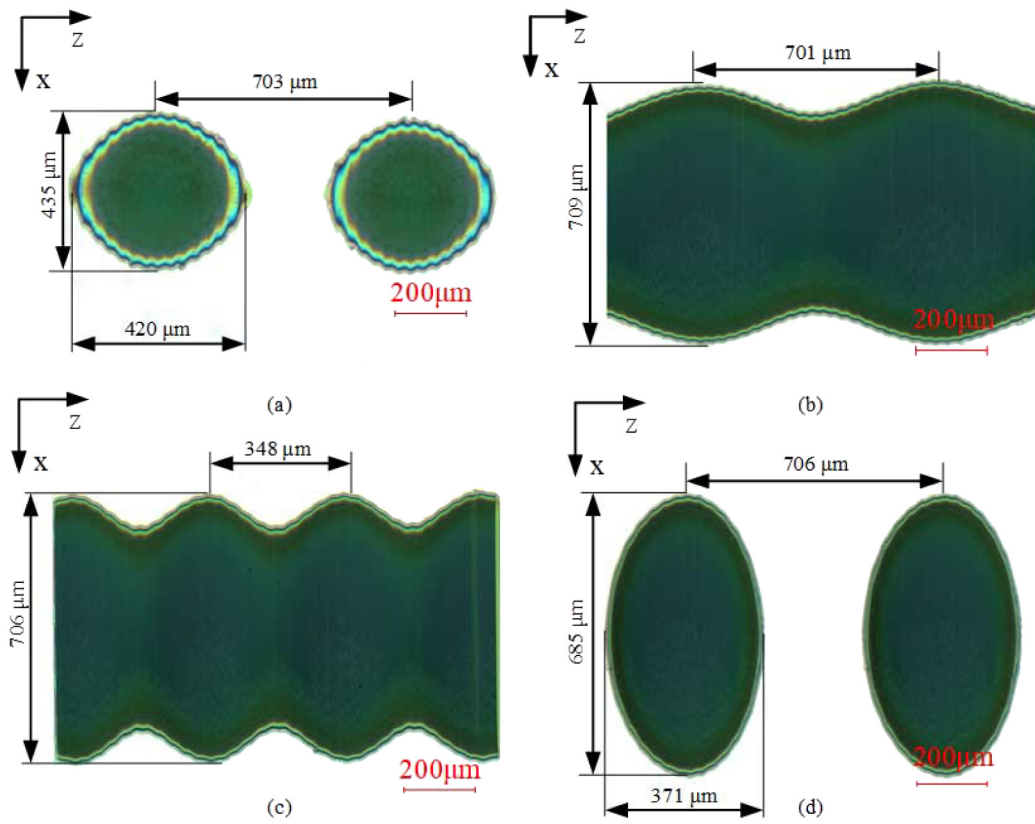


Fig. 15. Regulation of shape-controllable two-level structures by using the machining parameters labeled as (a) No. 1, (b) No. 2, (c) No. 3, (d) No. 4.

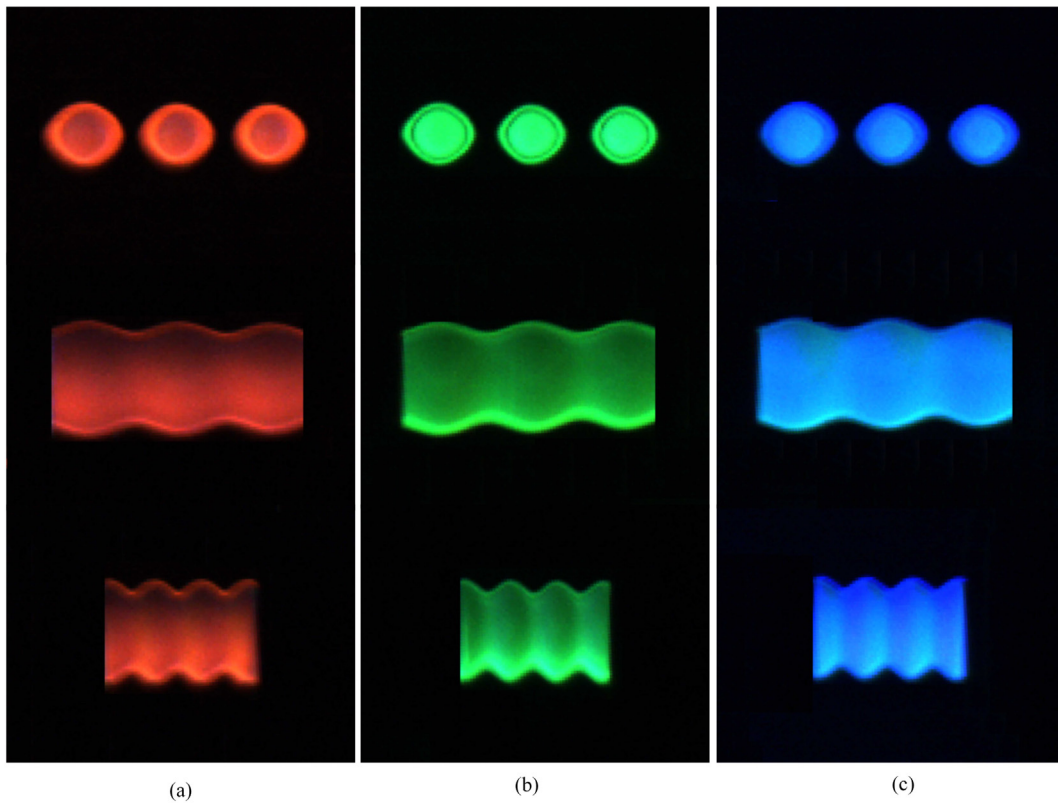


Fig. 16. Fabricated two-level iridescent structures at viewing angles of (a) 65°, (b) 55°, and (c) 45°.

first-order micro geometric features and the second-order sub-micron grooves.

- (2) A geometric model is established to design and fabricate the two-level iridescent structures, and the first-order geometric features corresponding to the shapes of the iridescent structures are precisely regulated by controlling the vibration parameters and the fly cutting condition.
- (3) The second-order submicron grooves with spacing covering the whole visible spectrum are precisely created and arrayed to form the feature of the first-order microstructures through VAFC. The high-saturation diffracted colors verify the precise manipulation of the second-order submicron grooves on the iridescent color.

Two-level iridescent structures show high saturation and uniformity, which proves the good color-rendering ability of the created two-level structures and is potentially applied to micro-optics, display devices and functional decoration.

CRediT authorship contribution statement

Yupeng He: Conceptualization, Methodology, Software, Writing - original draft. **Tianfeng Zhou:** Investigation, Data curation, Validation, Supervision. **Xiaobin Dong:** Writing - review & editing, Software. **Peng Liu:** Investigation. **Wenxiang Zhao:** Investigation. **Xibin Wang:** Investigation. **Yao Hu:** Investigation. **Jiawang Yan:** Supervision, Writing - review & editing.

Declaration of competing interest

The authors declare that they have no known competing financial interests or personal relationships that could have appeared to influence the work reported in this paper.

Acknowledgements

This work has been financed by the National Key Basic Research Program of China (No. 2015CB059900) and the National Natural Science Foundation of China (No. 51775046 & No. 51875043). The authors would also like to acknowledge the support from the Fok Ying-Tong Education Foundation for Young Teachers in the Higher Education Institutions of China (No. 151052).

Data availability

All data generated or analyzed are required to reproduce these findings are available and included in this article.

References

- [1] B. Dusser, Z. Sagan, H. Soder, N. Faure, J.P. Colombier, M. Jourlin, E. Audouard, Controlled nanostructures formation by ultra fast laser pulses for color marking, *Opt. Express* (2010) <https://doi.org/10.1364/oe.18.002913>.
- [2] K. Kumar, H. Duan, R.S. Hegde, S.C.W. Koh, J.N. Wei, J.K.W. Yang, Printing colour at the optical diffraction limit, *Nat. Nanotechnol.* (2012) <https://doi.org/10.1038/nnano.2012.128>.
- [3] J. Xue, Z.K. Zhou, Z. Wei, R. Su, J. Lai, J. Li, C. Li, T. Zhang, X.H. Wang, Scalable, full-colour and controllable chromotropic plasmonic printing, *Nat. Commun.* (2015) <https://doi.org/10.1038/ncomms9906>.
- [4] T. Ergin, N. Stenger, P. Brenner, J.B. Pendry, M. Wegener, Three-dimensional invisibility cloak at optical wavelengths, *Science* (80-.) (2010) <https://doi.org/10.1126/science.1186351>.
- [5] G. Tayeb, B. Gralak, S. Enoch, Structural colors in nature and butterfly-wing modeling, *Opt. Photonics News*. (2003) <https://doi.org/10.1364/opn.14.2.000038>.
- [6] J. Zi, X. Yu, Y. Li, X. Hu, C. Xu, X. Wang, X. Liu, R. Fu, Coloration strategies in peacock feathers, *Proc. Natl. Acad. Sci. U. S. A.* (2003) <https://doi.org/10.1073/pnas.2133313100>.
- [7] S. Kinoshita, S. Yoshioka, J. Miyazaki, Physics of structural colors, *Reports Prog. Phys.* (2008) <https://doi.org/10.1088/0034-4885/71/7/076401>.
- [8] Y. Yang, Y. Pan, P. Guo, Structural coloration of metallic surfaces with micro/nano-structures induced by elliptical vibration texturing, *Appl. Surf. Sci.* (2017) <https://doi.org/10.1016/j.apsusc.2017.01.026>.
- [9] D.T. Lindsey, Vision science: photons to phenomenology, *Optom. Vis. Sci.* (2000) <https://doi.org/10.1097/00006324-200005000-00008>.
- [10] A.D. Kersey, M.A. Davis, H.J. Patrick, M. LeBlanc, K.P. Koo, C.G. Askins, M.A. Putnam, E.J. Friebele, Fiber grating sensors, *J. Light. Technol.* (1997) <https://doi.org/10.1109/50.618377>.
- [11] D. Maystre, Diffraction gratings: an amazing phenomenon, *Comptes Rendus Phys* (2013) <https://doi.org/10.1016/j.crhy.2013.02.003>.
- [12] P.M. Van den Berg, Diffraction theory of a reflection grating, *Appl. Sci. Res.* (1971) <https://doi.org/10.1007/BF00411719>.
- [13] N. Bonod, J. Neauport, Diffraction gratings: from principles to applications in high-intensity lasers, *Adv. Opt. Photonics*. (2016) <https://doi.org/10.1364/aop.8.000156>.
- [14] C.-Y. Zhang, J.-W. Yao, H.-Y. Liu, Q.-F. Dai, L.-J. Wu, S. Lan, V.A. Trofimov, T.M. Lysak, Colorizing silicon surface with regular nanohole arrays induced by femtosecond laser pulses, *Opt. Lett.* (2012) <https://doi.org/10.1364/ol.37.001106>.
- [15] Y.C. Guan, W. Zhou, Z.L. Li, H.Y. Zheng, Femtosecond laser-induced iridescent effect on AZ31B magnesium alloy surface, *J. Phys. D: Appl. Phys.* (2013) <https://doi.org/10.1088/0022-3727/46/42/425305>.
- [16] H.D. Yang, X.H. Li, G.Q. Li, C. Wen, R. Qiu, W.H. Huang, J.B. Wang, Formation of colorized silicon by femtosecond laser pulses in different background gases, *Appl. Phys. A Mater. Sci. Process.* (2011) <https://doi.org/10.1007/s00339-011-6340-1>.
- [17] A.Y. Vorobyev, C. Guo, Colorizing metals with femtosecond laser pulses, *Appl. Phys. Lett.* (2008) <https://doi.org/10.1063/1.2834902>.
- [18] M.S. Ahsan, F. Ahmed, Y.G. Kim, M.S. Lee, M.B.G. Jun, Colorizing stainless steel surface by femtosecond laser induced micro/nano-structures, *Appl. Surf. Sci.* (2011) <https://doi.org/10.1016/j.apsusc.2011.04.027>.
- [19] X.D. Guo, R.X. Li, Y. Hang, Z.Z. Xu, B.K. Yu, H.L. Ma, B. Lu, X.W. Sun, Femtosecond laser-induced periodic surface structure on ZnO, *Mater. Lett.* (2008) <https://doi.org/10.1016/j.matlet.2007.09.082>.
- [20] R. Huang, X. Zhang, W.K. Neo, A.S. Kumar, K. Liu, Ultra-precision machining of grayscale pixelated micro images on metal surface, *Precis. Eng.* (2018) <https://doi.org/10.1016/j.precisioneng.2017.12.009>.
- [21] P. Guo, K.F. Ehmman, An analysis of the surface generation mechanics of the elliptical vibration texturing process, *Int. J. Mach. Tools Manuf.* (2013) <https://doi.org/10.1016/j.ijmactools.2012.08.003>.
- [22] Y. Yang, P. Guo, Global tool path optimization of high-resolution image reproduction in ultrasonic modulation cutting for structural coloration, *Int. J. Mach. Tools Manuf.* (2019) <https://doi.org/10.1016/j.ijmactools.2018.11.002>.
- [23] N. Suzuki, H. Yokoi, E. Shamoto, Micro/nano sculpturing of hardened steel by controlling vibration amplitude in elliptical vibration cutting, *Precis. Eng.* (2011) <https://doi.org/10.1016/j.precisioneng.2010.09.006>.
- [24] Z. Sun, S. To, K.M. Yu, One-step generation of hybrid micro-optics with high-frequency diffractive structures on infrared materials by ultra-precision side milling, *Opt. Express* (2018) <https://doi.org/10.1364/oe.26.028161>.
- [25] S. To, Z. Zhu, W. Zeng, Novel end-fly-cutting-servo system for deterministic generation of hierarchical micro-nanostructures, *CIRP Ann.* (2015) <https://doi.org/10.1016/j.cirp.2015.04.082>.
- [26] Z. Zhu, S. To, S. Zhang, Theoretical and experimental investigation on the novel end-fly-cutting-servo diamond machining of hierarchical micro-nanostructures, *Int. J. Mach. Tools Manuf.* (2015) <https://doi.org/10.1016/j.ijmactools.2015.04.002>.
- [27] Z. Ou, M. Huang, F. Zhao, Colorizing pure copper surface by ultrafast laser-induced near-subwavelength ripples, *Opt. Express* (2014) <https://doi.org/10.1364/oe.22.017254>.
- [28] X. Dong, T. Zhou, S. Pang, Z. Liang, B. Ruan, Z. Zhu, X. Wang, Mechanism of burr accumulation and fracture pit formation in ultraprecision microgroove fly cutting of crystalline nickel phosphorus, *J. Micromechanics Microengineering*. (2018) <https://doi.org/10.1088/1361-6439/aae8f9>.
- [29] S.J. Zhang, S. To, Z.W. Zhu, G.Q. Zhang, A review of fly cutting applied to surface generation in ultra-precision machining, *Int. J. Mach. Tools Manuf.* (2016) <https://doi.org/10.1016/j.ijmactools.2016.01.001>.
- [30] Y.C. Song, K. Nezu, C.H. Park, T. Moriwaki, Tool wear control in single-crystal diamond cutting of steel by using the ultra-intermittent cutting method, *Int. J. Mach. Tools Manuf.* (2009) <https://doi.org/10.1016/j.ijmactools.2008.10.014>.
- [31] J. Yan, T. Sasaki, J. Tamaki, A. Kubo, T. Sugino, Chip formation behaviour in ultra-precision cutting of electroless nickel plated mold substrates, *Key Eng. Mater.* 257-258 (2004) 3–8.